Chemical Science

Accepted Manuscript

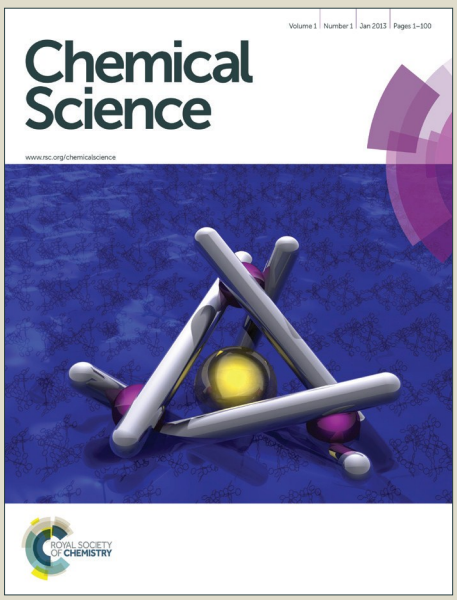

ROYAL SOCIETY OF CHEMISTRY

www.rsc.org/chemicalscience

Chemical Science

EDGE ARTICLE

Graphic abstract

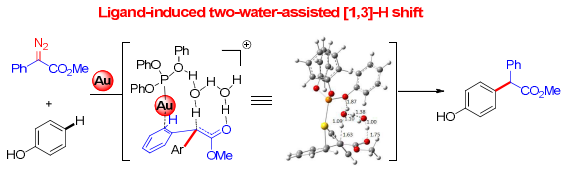

The origin of unique gold-catalyzed C-H functionalization of phenols with diazo compounds was disclosed by combined computational and experimental study.

Chemical Science

EDGE ARTICLE

Origins of Unique Gold-Catalysed Chemo- and Site-Selective C-H Functionalization of Phenols with Diazo Compounds

Received 00th January 20xx,
Accepted 00th January 20xx

DOI: 10.1039/x0xx00000x

www.rsc.org/

Yuan Liu,[ab‡] Zhunzhun Yu,[a‡] John Zenghui Zhang,[b] Lu Liu,*[a] Fei Xia,*[ab] and Junliang Zhang*[a]

In past decade, gold revealed more and more unique properties in carbene chemistry. It was disclosed by our recent communication (*J. Am. Chem. Soc.* **2014**, *136*, 6904.) that the gold carbenes have an unprecedented chemo- and site-selectivity and ligand effect toward the functionalization of C-H bond of phenols. In this full article, we report a comprehensively combined theoretical and experimental study on the mechanism of the insertion of gold carbenes into the C-H and O-H bonds in phenol. It significantly revealed that the ligands have an important effect on the C-H insertion and the reaction proceed through a pathway involving the formation of enolate-like intermediate. Moreover, two water molecules serving as a proton shuttle is believed to be the key issue for achieving the chemoselective C-H functionalization, which is strongly supported by the DFT calculations and control experiments. It is the first time to give a clear explanation about the prominent catalysis of gold carbenes toward C-H functionalization based on the theoretical and experimental study.

Introduction

Phenols are not only frequently found in natural products and pharmaceutics, but also powerful versatile platforms in organic synthesis.[1] Thus, the catalytic functionalization of phenols in a chemo- and site-selective manner is the most encompassing issue in organic chemistry.[2] In this context, the transition-metal-promoted decomposition of diazo compounds to generate metal carbenes has broad applications[3] in the direct site-selective functionalizations of phenols. In most cases, the O-H insertion takes place catalysed by a series of transition-metal catalysts such as copper, palladium, iron, and rhodium complexes.[4] In contrast, very recently, we and Shi independently found an unprecedented C(sp^2)-H bond functionalization of phenols with *α*-diazoesters,[5] furnishing *para*-substituted phenols **Pro-c8** via *para* C-H functionalization rather than the O-H insertion product **Pro-o8**. Meanwhile, the chemoselectivity is heavily dependent on the nature of ligand of gold catalyst[6] (Table 1). Although Nakamura and Pérez etc.[7] have theoretically studied the mechanism on the C(sp^3)-H insertion with carbene as well as Shi and co-workers[5b] analysed the electronic structures of gold carbenes by using the Density Functional Theory (DFT) calculations, no comprehensive mechanistic insight on the overall pathways of aromatic C(sp^2)-H insertion with carbene has been provided so far. To further understand the origin of this unique behaviour of gold carbene[8] in site selective C-H functionalization of phenol, we decided to carry out DFT calculations and experimental study to gain insights on the mechanism. Herein, we present a combined computational and experimental study to elucidate the origin of ligand effect on the chemoselectivity. Furthermore, the trace amount of water in the reaction mixture serving as a proton shuttle is proposed to be the key to give rise to the product **Pro-c8** of C-H insertion, which is supported by our current DFT calculations and control experiments.

Table 1. Various conditions.

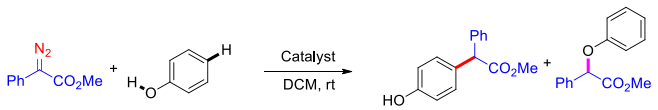

1 2 Pro-c8 Pro-o8

entry	Catalyst (5 mol%)	Time	Pro-c8[a]	Pro-o8[a]
1[b]	$Cu(OTf)_2$	5 min	0	11
2[b]	Cu(OTf)·toluene	5 min	0	9
3[b]	$[Pd(CH_3CN)_2Cl_2]$	12 h	0	33
4	$Fe(OTf)_2$	12 h	NR	
5[c]	$FeCl_2$	12 h	0	0
6[b]	$[Rh_2(OAc)_4]$	5 min	0	36
7	$Ph_3PAuSbF_6$	5 min	33	45
8	$(PhO)_3PAuSbF_6$	5 min	82	0

[a] NMR yield. [b] Then conversion of **1** is 100% and the major product is dimer of **1**. [c] Trace amount of dimer from **1** was detected.

[a] *Shanghai Key Laboratory of Green Chemistry and Chemical Processes, School of Chemistry and Molecular Engineering, East China Normal University, 3663 N. Zhongshan Road, Shanghai 200062, China, E-mail: lliu@chem.ecnu.edu.cn; fxia@chem.ecnu.edu.cn; jlzhang@chem.ecnu.edu.cn*
[b] *State Key Laboratory of Precision Spectroscopy, Institute of Theoretical and Computational Science & NYU-ECNU Center for Computational Chemistry at NYU Shanghai, 3663 Zhongshan Road North, Shanghai 200062, China.*
† Electronic Supplementary Information (ESI) available: Data for new compounds, experimental procedures and theoretical studies on mechanisms. For ESI and crystallographic data in CIF or other electronic format see DOI: 10.1039/x0xx00000x
‡ These authors contributed equally to this work

Chemical Science

EDGE ARTICLE

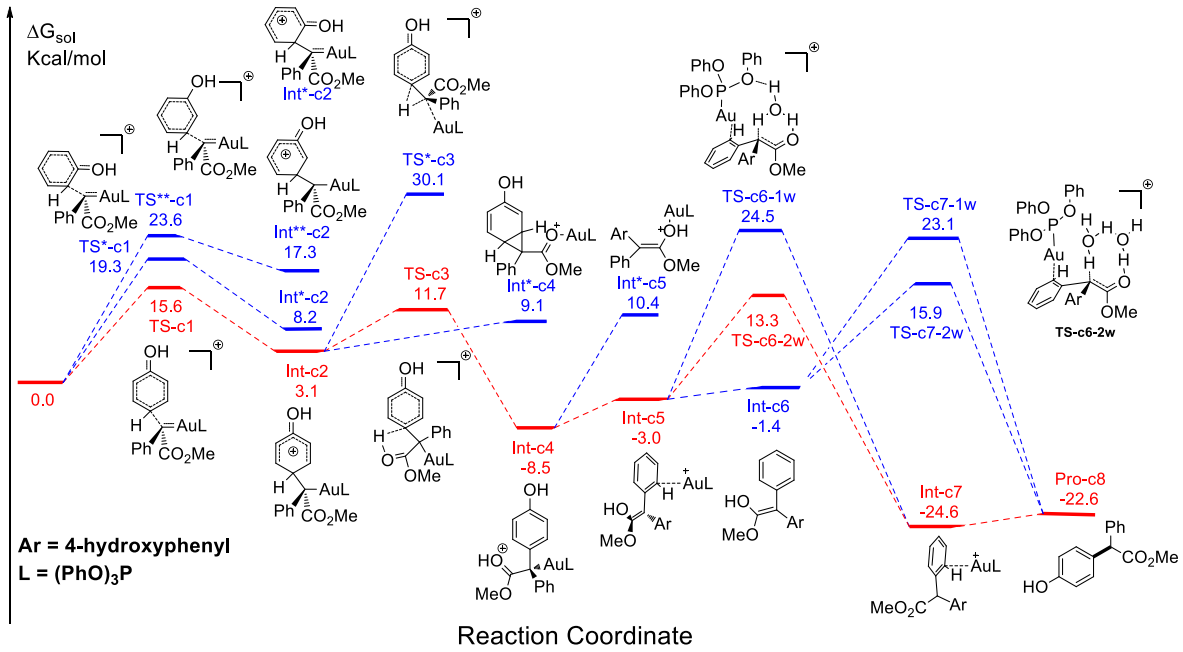

Figure 1. The calculated free energy profiles ΔG and the corresponding structures of intermediates and transition states along different possible C-H insertion pathways catalyzed by $(PhO)_3PAuSbF_6$. The reasonable pathways are shown in red and other possible pathways are in blue. All values of free energies are relative to the reactants of gold carbene and phenol and in the units of kcal/mol.

In the previous work on rhodium catalysed intramolecular aromatic C(sp^2)-H insertion reactions, Padwa and Doyle assumed that the reactions were triggered by the electrophilic addition of the metallocarbene intermediate to the aromatic ring, then followed by a [1,2]-H migration step.[9] Nevertheless, the reaction mechanisms for the prominent activity of gold carbenes toward C-H bonds still remain elusive. On the other hand, despite Yu and coworkers[10] have performed the mechanistic study of copper- and rhodium-catalysed O-H insertion of water with carbene using DFT calculations, the mechanism of gold-catalyzed O-H insertion has not yet been explored so far. In principle, there are three pivotal questions unsolved in this transformation: (1) Is the mechanism on the C(sp^2)-H insertion with gold carbenes as same as that of other metals such as rhodium? (2) What is the origin of ligand effect on the chemoselectivity? (3) Besides on the ligand, any other factors affect the chemoselectivity?

Computational Methods

All the DFT calculations were carried out in the Gaussian 09 software package.[11] The geometric structure of intermediates and transition states were optimized and located by using the M06 functional,[12] since the M06 functional has been demonstrated to generate accurate results for the organometallics especially in the description of noncovalent interactions. The Lanl2dz basis set[13] combined with the relativistic effective core potential for the inner electrons and double zeta basis for covalent electrons was used to describe the heavy elements Au and P, and the 6-31G* basis set[14] was used to describe the nonmetallic elements C, N, O and H. The frequency analyses were also performed based on the structures obtained in the gas phase to confirm that the intermediates are local minimum and the transition states have only one imaginary frequency. The intrinsic reaction coordinate (IRC) calculations[15] were performed to make sure that the crucial transition states connect the correct reactants and products. The solvent effect of CH_2Cl_2 was evaluated with the single point calculations using the integral equation formalism model (IEFPCM)[16] with the dielectric constant ε = 8.93 based on the structures in gas phase. All discussed energy values of intermediates and transition states throughout this paper are the Gibbs free energies in the units of kcal/mol that were calculated at the temperature 298 K, including the corrections of solvation free energies from the IEFPCM model. The 3D images of calculated structures were plotted using GaussView.[17] More structural details of intermediates and transition states can be found in the Supporting Information.

Results and discussion

On the pathway of C-H functionalization catalysed by $(PhO)_3PAuSbF_6$. It has been widely accepted that the metal catalysts could catalyse the diazo compounds to release N_2 and form reactive Au-carbenes, which were regarded as the precursors responsible for the C-H bonds insertions.[5,8a-e] To account for the generation of crucial precursors preceding C-H insertion, we calculated the reaction pathways of α-diazoesters and metal catalysts AuL (L=$(PhO)_3P$ and Ph_3P) in solution (Figure S1 of Supporting Information). The calculated free energy profiles indicate that the generation of Au-carbene species is quite facile and drastically exothermic, with the low barriers of 6.5 and 11.4 kcal/mol respectively. Therefore, the gold carbenes and phenol are regarded as the reactants for the subsequent C-H bond insertion reactions and the sum of their free energies is set as the benchmark, with the value of 0.0 kcal/mol.

Figure 1 displays the calculated free energy profiles for the C(sp^2)-H functionalization of phenol with gold carbene with the $(PhO)_3P$ as the ligand, where the structural details of intermediates and transition states are provided in Supporting Information. The previous theoretical investigations on the C(sp^3)-H insertions of rhodium, copper or silver carbenes, performed by Nakamura and Pérez, indicate that the first step of reactions involve the formation of σ-bond complexes of carbenes and the C(sp^3)-H bond.[7] Recently, Pérez and coworkers suggested that the mechanism of aromatic C(sp^2)-H bond insertion might be entirely different from that of aliphatic C(sp^3)-H bond insertion.[8c] In our DFT calculations, a transition state **TS-c1** with a barrier 15.6 kcal/mol is located for the addition of gold carbene at *para*-position of phenol. The **TS-c1** represents the transition state of direct C(sp^2)-C(sp^2) coupling of phenol and gold carbene, leading to the final *para*-C-H insertion product **Int-c2**. Accordingly, the addition of carbene at the *ortho* site of phenols gives rise to an intermediate **Int*-c2** with higher energy (8.2 kcal/mol vs **Int-c2**'s 3.1 kcal/mol) via the transition state **TS*-c1** with 19.3 kcal/mol. It is not surprising to find that the *meta*-position of phenol is the most unfavourable site for the addition with gold carbene, which needs an activation energy barrier up to 23.6 kcal/mol. Such high activation barriers of **TS*-c1** and **TS**-c1** prevent the carbenes from adding at the *ortho*- and *meta*-positions of phenol. The current DFT results are consistent with our experimental observations that the addition at the *para*-sites of substituted phenols was the predominant even with bulky steric hindrance (*i.e.*3, 5-dimethyl phenol).[5a] According to the previous calculations,[10] the intermediate **Int-c2** may be isomerize to the enolate via the mechanism of [1,3]-metal migration and yield a stable intermediate. However, it is found that such a stable

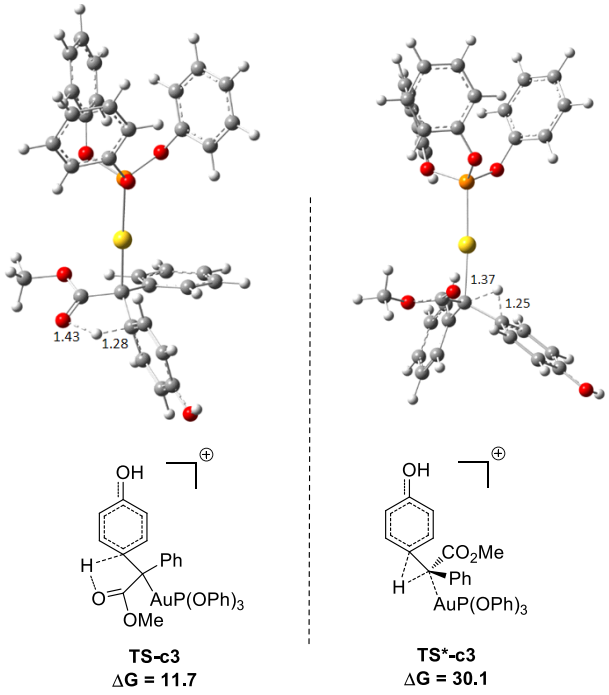

Figure 2. Optimized structures of transition states **TS-c3** and **TS*-c3** corresponding to Figure 1. The distances are in the units of angstroms and the values of free energies ΔG are in kcal/mol.

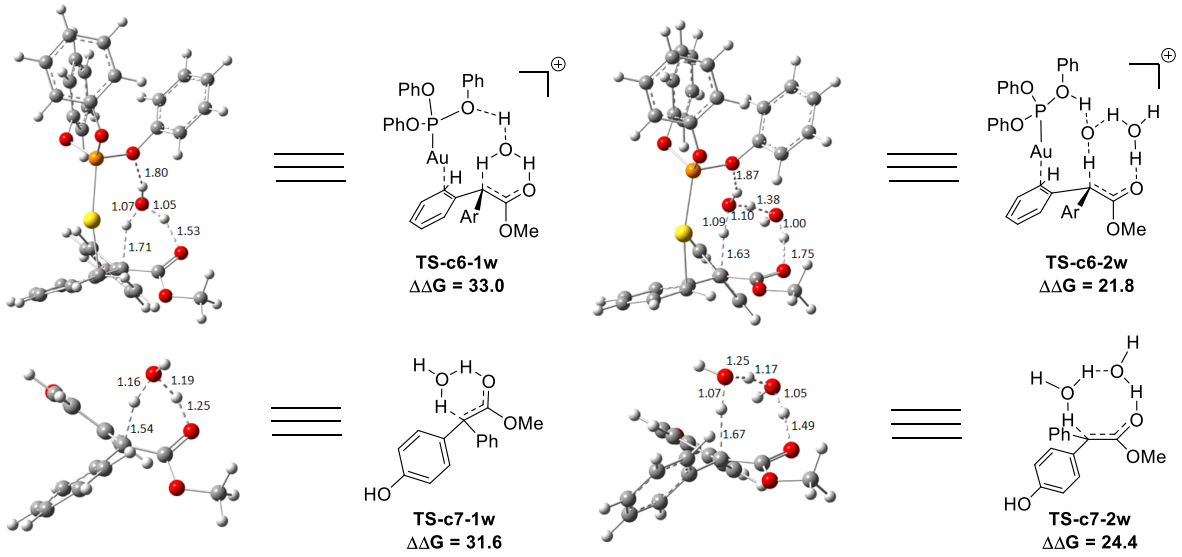

Figure 3. The structures of **TS-c6-1w**, **TS-c6-2w**, **TS-c7-1w** and **TS-c7-2w** in the pathways of C-H functionalization of phenol catalysed by $(PhO)_3PAuSbF_6$. The values of free energy barriers ΔΔG are in kcal/mol.

Chemical Science

EDGE ARTICLE

intermediate hardly exists after the [1,3]-Au migration in **Int-c2**, since a kind of cyclopropanation product of Büchner reaction is obtained, as shown by **Int*-c4**.[18] Meanwhile, this process of [1,3]-Au migration seems to be unfavorable in energetics, with the endothermicity of 9.1 kcal/mol to give **Int*-c4**. Additionally, in order to examine whether the commonly accepted mechanism of direct [1,2]-H shift is feasible, we located the transition state **TS*-c3** with the corresponding structure displayed in Figure 2. Our calculated results imply that **TS*-c3** has a considerable barrier of 30.1 kcal/mol, which could definitely rule out the mechanism of direct [1,2]-H shift in **Int-c2**. During the course of optimization, we happened to hypothesize that the carbonyl oxygen atom may intend to directly abstract the proton at the original *para*-site of phenol via a five-membered transition state **TS-c3** in Figure 2, to generate **Int-c4**. This process is quite facile according to the current calculations, merely with a small barrier 8.6 kcal/mol. Also, the **Int-c4** is more stable than **Int*-c4** by 17.6 kcal/mol. Subsequently, the intermediate **Int-c4** undergoes an unexpected isomerization to the enol **Int-c5** through a [1,3]-migration of the metal complex $(PhO)_3PAu^+$ to the phenyl ring rather than **Int*-c5**.

Two possible pathways might exist between the enol **Int-c5** and the final product **Pro-c8**. One is the gold-associated pathway, where the proton transfers through **TS-c6-1w** or **TS-c6-2w** to yield the intermediate **Int-c7**. Then, the metal complex $(PhO)_3PAu^+$ dissociates from **Int-c7** to yield **Pro-c8**. The other is the gold-free pathway, where the catalyst $(PhO)_3PAu^+$ firstly dissociates from **Int-c5** to yield the gold-free **Int-c6** and then proton transfer occurs via **TS-c7-1w** or **TS-c7-2w** to yield **Pro-c8**. As far as the two pathways are concerned, the key question is how the proton transfers from the hydroxyl to the final carbon in enol? In this work, we propose that the water in solvent plays a crucial role in undertaking the remote proton shuttle. Based on this proposal, we located the one-water assisted transition states **TS-c6-1w** and **TS-c7-1w**, as well as the two-water assisted transition states **TS-c6-2w** and **TS-c7-2w** along the reaction pathways, with the corresponding activation energy barriers of elementary steps displayed in Figure 3. The DFT results indicate that **TS-c6-1w** and **TS-c7-1w** involving one water molecule has higher energy barriers than that two-water assisted **TS-c6-2w** and **TS-c7-2w**. Figure 3 shows that the carboxyl group in **TS-c6-1w** and **TS-c7-1w** has to distort from the planar structures to form the hydrogen bonds with H_2O, but they still remain planar in **TS-c6-2w** and **TS-c7-2w**. The structural distortion in **TS-c6-1w** and **TS-c7-1w** might be the reason why they are in the high energy states. Interestingly, it is found that the oxygen atoms in the metal ligand $(PhO)_3P$ form hydrogen bonding interactions with the shuttle waters in **TS-c6-2w**, whereas it doesn't exist in another located transition state **TS*-c6-2w** (Figure S2 in Supporting Information). The calculated distance between the oxygen and hydrogen atom in **TS-c6-2w** of Figure 3 are 1.87 Å and its energy is 2.2 kcal/mol lower than that of **TS*-c6-2w**, indicating a possible stabilization effect of the metal complex $(PhO)_3PAu^+$ for the water chain in **TS-c6-2w**.

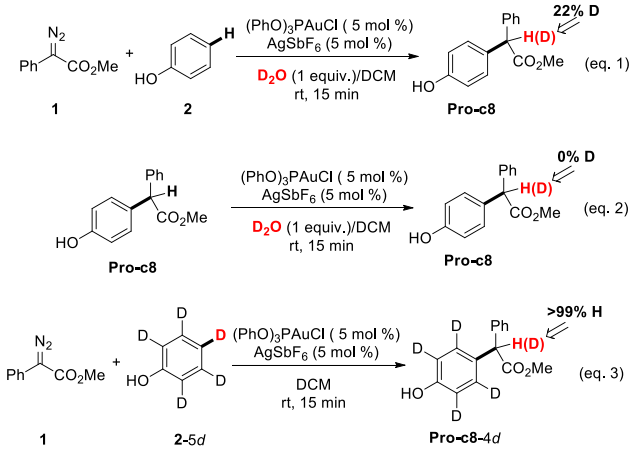

Scheme 1. Control experiments.

Control experiments were carried out in our lab (Scheme 1) to demonstrate the proposed mechanisms of gold carbene insertion into the C-H bond of phenol. When 1 equivalent of D_2O was added into the reaction system, and product **Pro-o8** was deuterated with the percentage of 22% (eq. 1). The relative low deuterium ratio might be attributed to the existence of trace amount of H_2O[19] that could also undertake the function of proton transfer. Additionally, it is well known that the hydrogen in the OH group of phenol could readily exchange with the deuterium in D_2O, which leads to the increased H_2O or DOH in solution. If a great number of H_2O participate in the process of proton shuttle, the ratio of deuterated product **Pro-o8** will definitely decrease. We also considered the possibility whether the phenols can serve as the proton shuttle. However, the calculated energy barrier between the transition state structure **TS-c6-2p** (Supporting Information) and **Int-c5** for the [1,3]-H shift is highly up to 36.1 kcal/mol, which implies it hardly occurs. The eq. 2 manifests that the direct proton exchange of **Pro-o8** with D_2O is impossible under the reaction conditions. More importantly, the eq.3 demonstrates that the reaction of **1** and deuterated phenol **2**-5*d* gives rise to the product **Pro-o8** without deuterium, which support the direct [1,2]-H shift[9] (**TS*-c3**) indeed does not occur in this case. The control experiments demonstrate that this kind of C-H bond insertion reactions governed by gold-carbene follows a novel mechanism involving water assisting process, rather than the previous commonly proposed direct [1,2]-H shift.[5,8a,8c, 9]

Chemical Science

EDGE ARTICLE

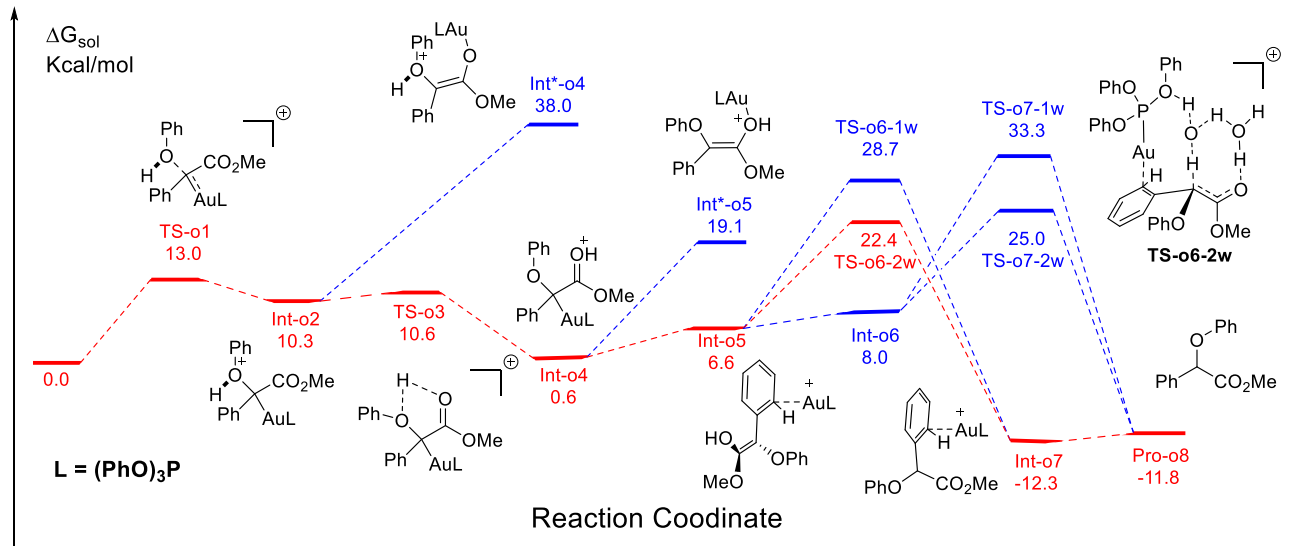

Figure 4. The calculated free energy profiles ΔG and corresponding structures of intermediates and transtion states along different possible O-H insertion pathways catalyzed by $(PhO)_3PAuSbF_6$. The reasonable pathway is shown in red and other possible pathways are in blue. All values of free energies are relative to the reactants of gold carbene and phenol and in the units of kcal/mol

Proposed pathway of O-H insertion catalysed by $(PhO)_3PAuSbF_6$. We next turn to address the question why the O-H insertion of phenol does not occur with the $(PhO)_3PAuSbF_6$ as the catalyst. In Figure 4, the calculated results show that an oxonium ylide[20] **Int-o2** formed through the **TS-o1** with a modest barrier. In the case of O-H bond insertion, a possible migration of complex LAu^+ to the carbonyl group in **Int-o2** is also taken into account, but the resulted structure **Int*-o4** is quite high in energy. The oxonium ylide **Int-o2** tends to isomerize to the more stable **Int-o4** via the **TS-o3**. The migration of gold catalyst to the phenyl group in **Int-o4** leads to the isomer **Int-o5**. It should note that **Int*-o5** is quite unstable in energetics, where the gold complex attaches to the oxygen atom in the hydroxyl group. Similar to the mechanism of C-H insertion in Figure 1, the rearrangements of **Int-o5** to **Pro-o8** pass through the gold-associated or gold-free pathways via the specific water-assisted transition states. We also locate the two-water assisted transition states **TS-o6-2w** for the gold-associated pathway and **TS-o7-2w** for the gold-free pathway, respectively (Figure 5). The activation barrier of **TS-o6-2w** (15.8 kcal/mol) is relatively lower that of **TS-o7-2w** (18.4 kcal/mol), indicate that the transformation of **Int-o5** to **Pro-o8** favours the gold-associated pathway via the **TS-o6-2w** rather than **TS-o7-2w**.

Rationale of the Chemoselectivity. Compared these two competitive reaction pathways in Figure 1 and Figure 4, it reveals that both two rearrangements from **Int-c5** or **Int-o5** to the final products are the rate-determining steps in the overall pathways, with the almost same total barriers of 21.8 kcal/mol. Nevertheless, the DFT calculations reveal that the thermal stability of intermediate of C-H insertion remarkably differs from that of O-H

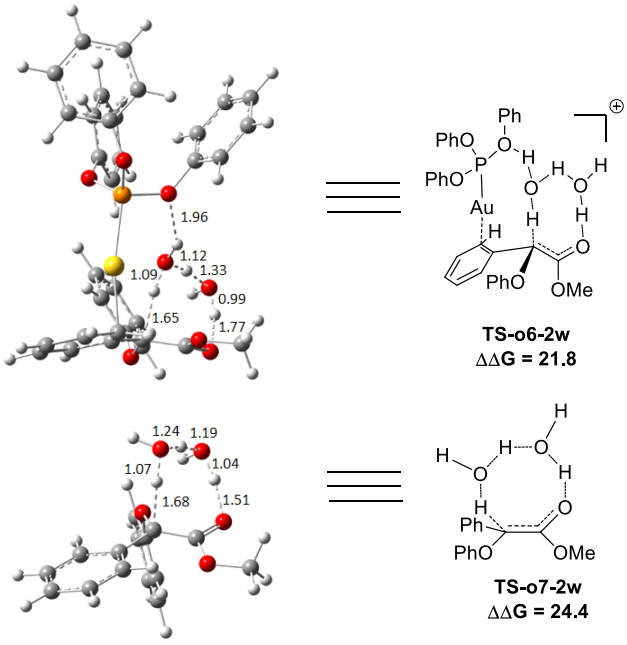

Figure 5. The structures of **TS-o6-2w** and **TS-o7-2w** in the proposed O-H functionalization of phenols catalysed by $(PhO)_3PAuSbF_6$. The distances are in the units of angstroms and the values of free energy barriers ΔΔG are in kcal/mol.

insertion. For example, the intermediate **Int-c4** is more stable than **Int-o4** by 9.1 kcal/mol, with the exothermic energy 8.5 kcal/mol. As for the final products, the energy of **Pro-c8** is 10.8 kcal/mol lower than the O-H insertion product **Pro-o8**. Besides, the endothermicity of **TS-c6-2w** is 13.3 kcal/mol, whereas the corresponding energy of **TS-o6-2w** is up to 22.4 kcal/mol relative to the sum of reactants. Such a large endothermicity of **TS-o6-2w** means that it is more difficult to pass through it to reach the product though the collision in solution. The calculated reaction pathways in Figure 1 and Figure 4 reveal that the stability of intermediates plays an important role in chemoselectivity and account for the unique chemoselectivity toward the C(sp^2)-H insertion.

In order to further understand the chemoselectivity, the reactions of phenol with α-phenyldiazoester catalysed by $(PhO)_3PAuSbF_6$ at different temperatures were also carried out. The ratios of **Pro-c8** : **Pro-o8** decreased from >20:1 to 2.5:1 along with lowering the reaction temperature from rt to -40 °C (Figure 6; For details, see Supporting Information). These results indicated that the C-H functionalization process was more favored at high temperature than low temperature. According to the free energy showed in Figure 1 and Figure 4, **Int-c4** and **Int-o4** should be the key intermediates for C-H functionalization and O-H insertion. As shown in Figure 6, **Int-c4** was more stable via higher barrier whilst **Int-o4** was more unstable via lower barrier. That is, the formation of **Int-c4** was the process of thermodynamic control, leading to the C-H functionalization. In contrast, the generation of **Int-o4** underwent kinetic control, leading to the O-H insertion. The control experiments at different temperatures and DFT calculations are in excellent consistency.

Two competitive pathways catalyzed by $Ph_3PAuSbF_6$. Additionally, the mechanisms of C-H and O-H insertions of phenol catalyzed by $Ph_3PAuSbF_6$ are also shown in Figure 6, with the corresponding barriers listed in Table 2. One hand, compared to the

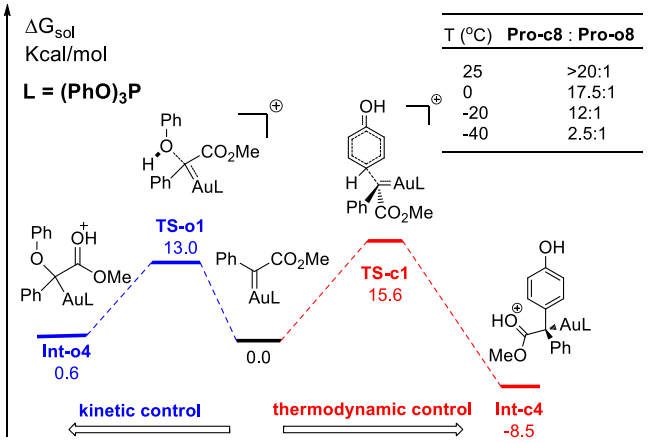

Figure 6. The reaction temperature on the chemoselectivity and the competitive pathways for the formation of two key intermediates. All values of free energies are relative to the reactants of gold carbene and phenol and in the units of kcal/mol.

corresponding pathways in Figure 1 and Figure 4, we found that the ligand Ph_3P has a remarkable electronic effect on the change of dynamics barriers of electrophilic addition to intermediates **Int-o12** and **Int-c12**. For the C-H insertion, the addition barrier via **TS-c9** was enhanced to be 18.2 kcal/mol, with 2.6 kcal/mol higher than that of **TS-c1**. In contrast, the barrier of O-H insertion via **TS-o9** lowers from 13.0 to 11.8 kcal/mol. It is no doubt that the change of the barriers of addition is disadvantageous to the C-H insertion but advantageous to O-H insertion. On the other hand, the calculated barrier of hydrogen transfer via **TS-o15-2w** in O-H insertion is 18.0 kcal/mol, relatively lower than the barrier of 22.0 kcal/mol C-H insertion. Therefore, the reaction of C-H insertion shown in Figure 6 is significantly slowed down in comparison to the case catalysed by

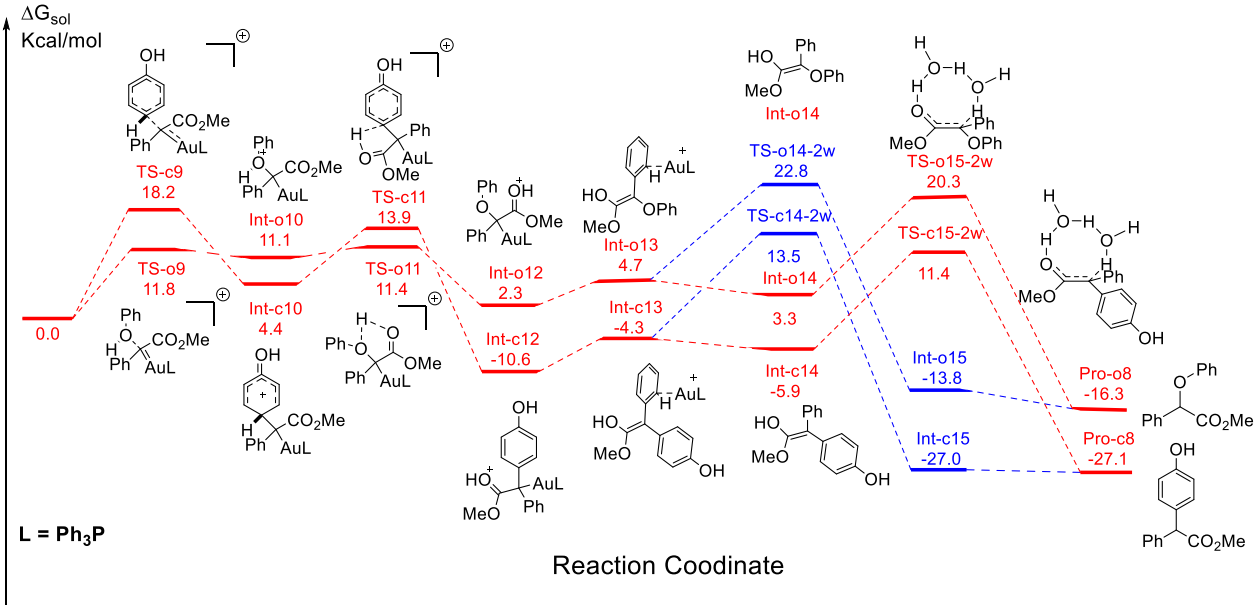

Figure 7. The competitive pathways of C-H and O-H insertion catalyzed by $Ph_3PAuSbF_6$. The two reasonable pathways are shown in red and other possible pathways in blue. All values of free energies are relative to the reactants of gold carbenes and phenol and in the units of kcal/mol.

Chemical Science

EDGE ARTICLE

$(PhO)_3PAuSbF_6$ in Figure 1. Products of C-H insertions are still more stable than the counterparts of O-H insertion in thermodynamics according to the current DFT calculations. Considering both the dynamic and thermodynamic effects, the calculated pathways could account for the low chemoselectivity for **Pro-c8** and **Pro-o8** catalysed by $Ph_3PAuSbF_6$ that has been observed in our experiments.

Table 2. The calculated free energetic spans ΔΔG of hydrogen transfer through transition states (TSs) assisted by one water and two water molecules in Figure 6. The values of ΔΔG are in the units of kcal/mol.

TSs	TS-c14-2w	TS-c15-2w	TS-o14-2w	TS-o15-2w
ΔΔG	24.1	22.0	20.5	18.0

Conclusions

In summary, the origin of unique chemoselectivity of C-H bond functionalization of phenol with diazo compounds catalyzed by $(PhO)_3PAuSbF_6$ is due to its high thermodynamic stability of intermediates and products, as well as the modest energy barrier of the rate-determining step. It is the first time to propose that the reactions of gold carbenes with phenol pass through the specific pathways involving the formation of stable enol. The hydrogen transfers in the rearrangements from enol to final products follow a novel reaction pathway with the two water molecules serving as a proton shuttle rather than the previous commonly proposed direct [1,2]-H shift. The DFT calculations also reveal that the oxygen atoms in the ligand $(PhO)_3P$ play an important role in stabilizing the transition states of hydrogen transfer. The observed ligand effects of metal complexes on the reaction pathways are well rationalized based on the results of present DFT calculations. The novel mechanistic insights delineated above will refine the model of gold catalyst in carbene chemistry and contribute to the future development of this field as well as the rational designing in chemo- and site-selective organic transformation.

Acknowledgements

Financial support by the 973 Program (2011CB808600), Shanghai Pujiang Program (14PJ1403100), National Natural Science Foundation of China (21572065, 21433004, 21473056, 21425205), Changjiang Scholars and Innovative Research Team in University (PCSIRT) are greatly appreciated. We acknowledge the support of the NYU-ECNU Center for Computational Chemistry at NYU Shanghai.

Notes and references

1 *Synthetic and Natural Phenols*, ed. J. H. P. Tyman, Elsevier, 1996.

2 For recent highlights, see: (a) D.-G. Yu, F. de Azambuja and F. Glorius, *Angew. Chem. Int. Ed.*, 2014, **53**, 7710; (b) P. MacLellan, *Nat. Chem.*, 2014, **6**, 375; For selected examples, see: (c) R. B. Bedford, S. J. Coles, M. B. Hursthouse and M. E. Limmert, *Angew. Chem. Int. Ed.*, 2003, **42**, 112; (d) R. B. Bedford and M. E. Limmert, *J. Org. Chem.*, 2003, **68**, 8669; (e) J. Luo, S. Preciado and I. Larrosa, *J. Am. Chem. Soc.*, 2014, **136**, 4109; (f) R. Zhu, J. Wei and Z.-J. Shi, *Chem. Sci.*, 2013, **4**, 3706; (g) Z. Huang, L. Jin, Y. Feng, P. Peng, H. Yi and A. Lei, *Angew. Chem. Int. Ed.*, 2013, **52**, 7151; (h) Z. Wu, F. Luo, S. Chen, Z. Li, H. Xiang and X. Zhou, *Chem. Commun.*, 2013, **49**, 7653; (i) H.-X. Dai, G. Li, X.-G. Zhang, A. F. Stepan and J.-Q. Yu, *J. Am. Chem. Soc.*, 2013, **135**, 7567; (j) A. Seoane, N. Casanova, N. Quiñones, J. L. Mascareñas and M. Gulías, *J. Am. Chem. Soc.*, 2014, **136**, 834; (k) Y. E. Lee, T. Cao, C. Torruellas and M. C. Kozlowski, *J. Am. Chem. Soc.*, 2014, **136**, 6782; (l) C. S. Sevov and J. F. Hartwig, *J. Am. Chem. Soc.*, 2013, **135**, 9303; (m) K. V. N. Esguerra, Y. Fall, L. Petitjean and J.-P. Lumb, *J. Am. Chem. Soc.*, 2014, **136**, 7662; (n) Y. Kuninobu, T. Matsuki and K. Takai, *J. Am. Chem. Soc.*, 2009, **131**, 9914; (o) C.-L. Ciana, R. J. Phipps, J. R. Brandt, F.-M. Meyer and M. J. Gaunt, *Angew. Chem. Int. Ed.*, 2011, **50**, 458.

3 For selected reviews, see: (a) *Modern Catalytic Methods for Organic Synthesis with Diazo Compounds: From Cyclopropanes to Ylides*, ed. M. P. Doyle, M. A. McKervey and T. Ye, Wiley-VCH, New York, 1998; (b) M. P. Doyle, R. Duffy, M. Ratnikov and L. Zhou, *Chem. Rev.*, 2010, **110**, 704; (c) H. M. L. Davies and Y.-J. Lian, *Acc. Chem. Res.*, 2012, **45**, 923; (d) H. M. L. Davies and D. Morton, *Chem. Soc. Rev.*, 2011, **40**, 1857; (e) M. M. Díaz-Requejo and P. J. Pérez, *Chem. Rev.*, 2008, **108**, 3379; (f) Z. Liu and J. Wang, *J. Org. Chem.*, 2013, **78**, 10024.

4 For reviews, see: (a) D. Gillingham and N. Fei, *Chem. Soc. Rev.*, 2013, **42**, 4918; (b) X. Guo and W. Hu, *Acc. Chem. Res.*, 2013, **46**, 2427; (c) S.-F. Zhu and Q.-L. Zhou, *Acc. Chem. Res.*, 2012, **45**, 1365; (d) D. J. Miller and C. J. Moody, *Tetrahedron*, 1995, **51**, 10811. For selected examples, see: (e) P. Yates, *J. Am. Chem. Soc.*, 1952, **74**, 5376; (f) Z. Zhu and J. H. Espenson, *J. Am. Chem. Soc.*, 1996, **118**, 9901; (g) Z. Qu, W. Shi and J. Wang, *J. Org. Chem.*, 2004, **69**, 217; (h) Z. Zhang, Y. Liu, L. Ling, Y. Li, Y. Dong, M. Gong, X. Zhao, Y. Zhang and J. Wang, *J. Am. Chem. Soc.*, 2011, **133**, 4330; (i) J. R. Sosa, A. A. Tudjarian and T. G. Minehan, *Org. Lett.*, 2008, **10**, 5091; (j) K. J. Kilpin, U. S. D. Paul, A.-L. Lee and J. D. Crowley, *Chem. Commun.*, 2011, **47**, 328; (k) R. A. Maurya, C. P. Park, J. H. Lee and D.-P. Kim, *Angew. Chem. Int. Ed.*, 2011, **50**, 5952; (l) T. Osako, D. Panichakul and Y. Uozumi, *Org. Lett.*, 2012, **14**, 194; (m) K. B. S. Magar and Y. R. Lee, *Org. Lett.*, 2013, **15**, 4288. For asymmetric version, see: (n) T. C. Maier and G. C. Fu, *J. Am. Chem. Soc.*, 2006, **128**, 4594; (o) C. Chen, S.-F. Zhu, B. Liu, L.-X. Wang and Q.-L. Zhou, *J. Am. Chem. Soc.*, 2007, **129**, 12616; (p) X.-L. Xie, S.-F. Zhu, J.-X. Guo, Y. Cai and Q.-L. Zhou, *Angew. Chem. Int. Ed.*, 2014, **53**, 2978.

5 (a) Z. Yu, B. Ma, M. Chen, H.-H. Wu, L. Liu and J. Zhang, *J. Am. Chem. Soc.*, 2014, **136**, 6904; (b) Y. Xi, Y. Su, Z. Yu, B. Dong, E.

J. McClain, Y. Lan and X. Shi, *Angew. Chem. Int. Ed.*, 2014, **53**, 9817.

6 For selected recent accounts and general reviews, see: (a) A. Corma, A. Leyva-Perez and M. J. Sabater, *Chem. Rev.*, 2011, **111**, 1657; (b) C. Aubert, L. Fensterbank, P. Garcia, M. Malacria and A. Simonneau, *Chem. Rev*., 2011, **111**, 1954; (c) N. Krause and C. Winter, *Chem. Rev*., 2011, **111**, 1994; (d) M. Bandini, *Chem. Soc. Rev*., 2011, **40**, 1358; (e) B.-L. Lu, L. Dai and M. Shi, *Chem. Soc. Rev.*, 2012, **41**, 3318; (f) D. Garayalde and C. Nevado, *ACS Catal*., 2012, **2**, 1462; g) Y. -W. Sun, Q. Xu and M. Shi, *Beilstein J. Org. Chem.*, 2013, **9**, 2224; (h) F. López and J. L. Mascareñas, *Beilstein J. Org. Chem.*, 2013, **9**, 2250; (i) G. Cera and M. Bandini, *Isr. J. Chem.*, 2013, **53**, 848; (j) W. Yang and A. S. K. Hashmi, *Chem. Soc. Rev.,* 2014*,* **43***,* 2941; (k) F. López and Mascareñas, J. *Chem. Soc. Rev.*, 2014, **43**, 2904; (l) C. Obradors and A. M. Echavarren, *Acc. Chem. Res.*, 2014, **47**, 902; (m) A. S. K. Hashmi, *Acc. Chem. Res.,* 2014, **47**, 864; (n) L. Zhang, *Acc. Chem. Res.*, 2014, **47**, 877; (o) F. López and J. L. Mascareñas, *Beilstein J. Org. Chem.*, 2011, **7**, 1075; (p) D. Qian and J. Zhang, *Chem. Rec.* 2014, **14**, 280; (q) D. Qian and J. Zhang, *Chem. Soc. Rev.* 2015, **44**, 677.

7 (a) E. Nakamura, N. Yoshikai and M. Yamanaka, *J. Am. Chem. Soc.*, 2002, **124**, 7181; (b) A. A. C. Braga, F. Maseras, J. Urbano, A. Caballero, M. M. Díaz-Requejo and P. J. Pérez, *Organometallics*, 2006, **25**, 5292.

8 For gold-catalyzed carbene transfer from diazo compounds, see: (a) M. R. Fructos, T. R. Belderrain, P. de Frémont, N. M. Scott, S. P. Nolan, M. M. Díaz-Requejo and P. J. Pérez, *Angew. Chem. Int. Ed.*, 2005, **44**, 5284; (b) M. R. Fructos, P. de Frémont, S. P. Nolan, M. M. Díaz-Requejo and P. J. Pérez, *Organometallics*, 2006, **25**, 2237; (c) I. Rivilla, B. P. Gõmez-Emeterio, M. R. Fructos, M. M. Díaz-Requejo and P. J. Pérez, *Organometallics*, 2011, **30**, 2855; (d) E. López, G. Lonzi and L. A. López, *Organometallics*, 2014, **33,** 5924; (e) J. Barluenga, G. Lonzi, M. Tomás and L. A. López, *Chem. Eur. J.*, 2013, **19**, 1573; (f) J. F. Briones and H. M. L. Davies, *J. Am. Chem. Soc.*, 2012, **134**, 11916; (g) J. F. Briones and H. M. L. Davies, *J. Am. Chem. Soc.*, 2013, **135**, 13314; (h) Z.-Y. Cao, X. Wang, C. Tan, X.-L. Zhao, J. Zhou and K. Ding, *J. Am. Chem. Soc.*, 2013, **135**, 8197; (i) V. V. Pagar, A. M. Jadhav and R. S. Liu, *J. Am. Chem. Soc.*, 2011, **133**, 20728; (j) A. M. Jadhav, V. V. Pagar and R.-S. Liu, *Angew. Chem. Int. Ed.*, 2012, **51**, 11809; (k) S. K. Pawar, C.-D. Wang, S. Bhunia, A. M. Jadhav and R.-S. Liu, *Angew. Chem. Int. Ed.*, 2013, **52**, 7559; (l) D. Zhang, G. Xu, D. Ding, C. Zhu, J. Li and J. Sun, *Angew. Chem. Int. Ed.*, 2014, **53**, 11070; (m) G. Xu, C. Zhu, W. Gu, J. Li and J. Sun, *Angew. Chem. Int. Ed.*, 2015, **54**, 883; (n) Y. Zhou, B. G. Trewyn, R. J. Angelici and L. K. Woo, *J. Am. Chem. Soc.*, 2009, **131**, 11734; (o) G. Lonzi and L. A. López, *Adv. Synth. Catal.*, 2013, **355**, 1948; (p) A. Prieto, M. R. Fructos, M. M. Díaz-Requejo, P. J. Pérez, P. Pérez-Galán, N. Delpont and A. M. Echavarren, *Tetrahedron*, 2009, **65**, 1790.

9 A. Padwa, D. J. Austin A. T. Price, M. A. Semones, M. P. Doyle, M. N. Protopopova, W. R. Winchester and A. Tran, *J. Am. Chem. Soc.*, 1993, **115**, 8669.

10 Y. Liang, H. Zhou and Z.-X. Yu, *J. Am. Chem. Soc.*, 2009, **131**, 17783.

11 M. J. Frisch, G. W. Trucks, H. B. Schlegel, G. E. Scuseria, M. A. Robb, J. R. Cheeseman, G. Scalmani, V. Barone, B. Mennucci, G. A. Petersson, H. Nakatsuji, M. Caricato, X. Li, H. P. Hratchian, A. F. Izmaylov, J. Bloino, G. Zheng, J. L. Sonnenberg, M. Hada, M. Ehara, K. Toyota, R. Fukuda, J. Hasegawa, M. Ishida, T. Nakajima, Y. Honda, O. Kitao, H. Nakai, T. Vreven, J. A. Montgomery, Jr., J. E. Peralta, F. Ogliaro, M. Bearpark, J. J. Heyd, E. Brothers, K. N. Kudin, V. N. Staroverov, R. Kobayashi, J. Normand, K. Raghavachari, A. Rendell, J. C. Burant, S. S. Iyengar, J. Tomasi, M. Cossi, N. Rega, J. M. Millam, M. Klene, J. E. Knox, J. B. Cross, V. Bakken, C. Adamo, J. Jaramillo, R. Gomperts, R. E. Stratmann, O. Yazyev, A. J. Austin, R. Cammi, C. Pomelli, J. W. Ochterski, R. L. Martin, K. Morokuma, V. G. Zakrzewski, G. A. Voth, P. Salvador, J. J. Dannenberg, S. Dapprich, A. D. Daniels, Ö. Farkas, J. B. Foresman, J. V. Ortiz, J. Cioslowski and D. J. Fox, *Gaussian 09*, Revision B.01; Gaussian, Inc.: Wallingford CT, 2009.

12 (a) Y. Zhao and D. G. Truhlar, *Theor. Chem. Acc.*, 2008, **120**, 215; (b) Y. Zhao and D. G. Truhlar, *Acc. Chem. Rec.*, 2008, **41**, 157.

13 (a) P. J. Hay and W. R. Wadt *J. Chem. Phys.*, 1985, **82**, 299; (b) W. R. Wadt and P. J. Hay, *J. Chem. Phys.*, 1985, **82,** 284.

14 V. A. Rassolov, M. A. Ratner, J. A. Pople, P. C. Redfern and L. A. Curtiss, *J. Chem. Phys*., 2001, **22**, 976.

15 K. Fukui, *Acc. Chem. Res.*, 1981, **14**, 363.

16 G. Scalmani and M. J. Frisch, *J. Chem. Phys*., 2010, **132**, 114110.

17 R. Dennington, T. Keithm and J. Millam, *GaussView*, Version 5, Semichem Inc.: Shawnee Mission, KS, 2009.

18 In order to rule out the pathway via Büchner reaction, more control experiments were also carried out in our lab. Please see section 3 in supporting information for more details.

19 Y. Xia, Y. Liang, Y. Chen, M. Wang, L. Jiao, F. Huang, S. Liu, Y. Li and Z.-X. Yu, *J. Am. Chem. Soc.*, 2007, **129**, 3470.

20 For a nice experiment example of O-H insertion via oxonium ylide, see: X. Zhang, H. Huang, X. Guo, X. Guan, L. Yang and W. Hu, *Angew. Chem. Int. Ed*., 2008, **47**, 6647.